EVOLUTIONARY OPTIMIZATION OF TCO/MESH ELECTRICAL CONTACTS IN CIGS SOLAR CELLS

Paolo A. Losio[1*], Thomas Feurer[2], Stephan Buecheler[2], Beat Ruhstaller[1]
[1] Zurich University of Applied Sciences (ZHAW), School of Engineering, Institute of Computational Physics, Technikumstr. 9, 8401 Winterthur, Switzerland.
[2] Laboratory for Thin films and Photovoltaics, Empa, Swiss Federal Laboratories for Materials Science and Technology, Ueberlandstrasse 129, 8600 Dübendorf, Switzerland
* Corresponding author, paolo.losio@zhaw.ch

ABSTRACT:
State of the art solar cells often require a combination of TCO and metallic grid to efficiently transport the generated current to an external circuit. Optimization of these complex contacts based on several materials with different conductivities and geometries is often still based on a traditional approach consisting of simple analytical formulas and empirical knowledge in spite of the complexity. An evolutionary algorithm combined with an electrical 2D+1D FEM model is used to optimize the shape of the metallic contact considering the material conductivities, the geometry and shadowing.
The performance of two automatically designed contacts is compared with experimental results of CIGS solar cells prepared with two different TCO thicknesses.
Keywords: Thin Film, Modelling, Contact, Metal Grid

1 INTRODUCTION

Cu(In, Ga)Se_2 (CIGS) thin film solar cells are promising for large scale efficient PV applications.[1] Collecting and transporting the current generated in CIGS solar cells is a key factor for performance optimization in record devices as well as a critical issue in scaling to large area. Especially CIGS modules, characterized by a comparatively low cell V_{oc} and comparatively high J_{sc} are affected by strong ohmic losses. Therefore minimizing ohmic losses is of paramount importance. Usually the current is transported through a window TCO layer and in recent times a metallic mesh is added for improving the overall conductivity and reducing ohmic losses.

Modelling a solar cell based only on single TCO layers as contacts can be easily achieved by using equivalent circuits in SPICE [2] however adding a highly conductive metallic mesh on top of the TCO makes a simulation by equivalent circuits more complex because a two dimensional spatial discretization is required and the direction of current flow cannot be accurately described [3]. As an alternative it is possible to use the finite element method (FEM) to describe the potential distribution and the current flow in an extended device comprising both TCO and a metallic grid. [4–6]

A common approach to optimize contacting grids and module interconnection layouts is based on analytical models [7,8] relying on several approximations that may hold for simple geometries only. More advanced approaches based on FEM have been used only since recently.[5,9]

2 SIMULATION AND OPTIMIZATION

Simulations using the finite elements method are performed using the Multiphysics FEM package nm-seses developed at ZHAW.[4,10] In the present study the solar cell is decomposed into three 2D domains: a bottom Mo electrode, a top TCO electrode and a metallic grid as shown in Fig. 1. The solar cell is modelled using a one diode model implemented as a one dimensional coupling between Mo and the top TCO, e.g. each mesh point node between top TCO and Mo is connected through a one diode model. The metallic contact grid is modelled as a square mesh where each element can either be metal or void, and the top metal electrode is in perfect contact with the top TCO layer. The presence of a metal mesh element induces a shadowing into the solar cell model, e.g. the photocurrent is locally set to zero. Dirichlet boundary conditions (BC) with voltage = 0V are applied to the bottom Mo electrode, and similarly Dirichlet BC with a voltage corresponding to the external voltage are applied to the edges of a contact pad on the metallic mesh. All other boundaries are defined as insulating. Existing (e.g. experimental) metallic contact grids can be imported as bitmapped images to allow calculating the cell performance.

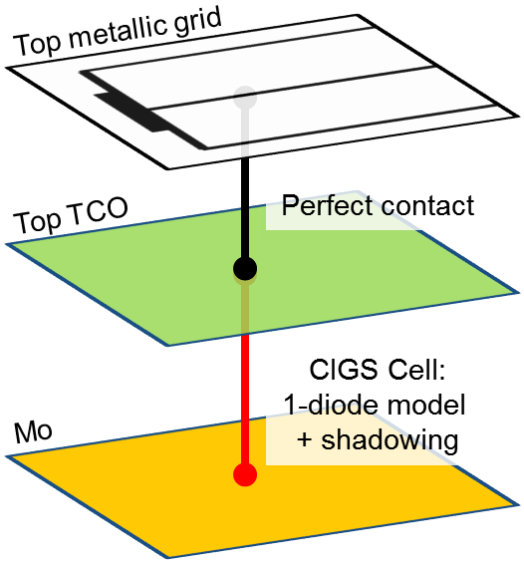

Figure 1 Schematic representation of the model geometry, dimensionality and couplings.

The parameters of the one diode model used for the simulations are obtained by fitting an experimentally measured IV curve. In a first pass the parameters are fitted using a simple one diode model, and then these initial val-

ues are used for accurate fitting based on a full FEM model to accurately take into account the potential distribution across a device. The measured resistivity of Al doped Zinc oxide (AZO, $1.1 \cdot 10^{-3}$ Ωcm) and Mo ($1.2 \cdot 10^{-5}$ Ωcm) together with tabulated data for Al ($2.7 \cdot 10^{-6}$ Ωcm) are used for all calculations. Parasitic losses in the TCO layer were estimated by extracting the absorption coefficient of AZO from measured transmission and reflection spectra.

In principle it is possible to automatically optimize the topology and the shape of metallic contacting grids by using topology optimization algorithms used e.g. in civil engineering but adapted to the problem of efficiently collecting current from a surface minimizing shadowing. An intuitive optimization method is the "Bidirectional Evolutionary Structural Optimization" (BESO) method [11] which can be easily adapted to optimize electrical contacts. The optimization algorithm iteratively adds metal mesh elements to the top electrode at points where the ohmic losses in the top TCO layer are highest. This approach is repeated until gains in current collection are compensated by losses due to shadowing and the efficiency of the cell cannot be increased any more. As a successive step, the metallic contacts are iteratively thinned to minimize shadowing losses taking care of not impairing current collection. As this optimization method finds only local minima, it is necessary to repeat the optimization several times and slightly modify the number of metal mesh elements added at each iteration.

The contacts presented in this study were obtained starting from a 0.5x1 cm^2 simulation domain using a resolution of 40 µm defined by the equipment used to produce the shadow masks. Minor modifications allow to apply the optimization method to large area modules.

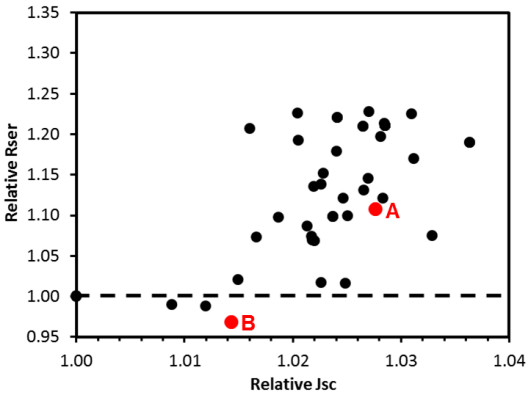

Figure 2: Summary of the improvements in the apparent serial resistance (R_{ser}) and short circuit current (J_{sc}) obtained in about 50 optimization runs for solar cells of 0.5 cm^2 surface. The two contacts (A, B) marked by red dots were realized experimentally.

3 EXPERIMENTS AND RESULTS

CIGS solar cells were prepared at Empa using the procedure described elsewhere.[1,12] Metallic contacts were prepared by evaporation of 4 µm Al through a shadow mask. Shadow masks were prepared by laser-cutting a 100 µm Mo foil according to two grid designs computed by the optimization tool, the nominal dimensions of the experimentally realized cells were 0.54x1.07 cm^2 and are slightly larger than the computed designs. The computed designs were stretched to match the target dimensions and a future optimization series will take into account the new dimensions.

About 50 optimization runs were done using slightly different thresholds for metal addition and different locations of the contact pad to explore the possibilities offered by this method. A standard metallic contact grid was used as benchmark: the results are summarized in Fig. 2 indicating the relative changes in short circuit current (J_{sc}) and in apparent series resistance (R_{ser}) which could be achieved in each run. Ideally, an optimized contact geometry allows reducing the serial resistance and increasing the short circuit current. However, most of the contact shapes lead to an improvement of J_{sc} at cost of a slight increase of R_{ser}.

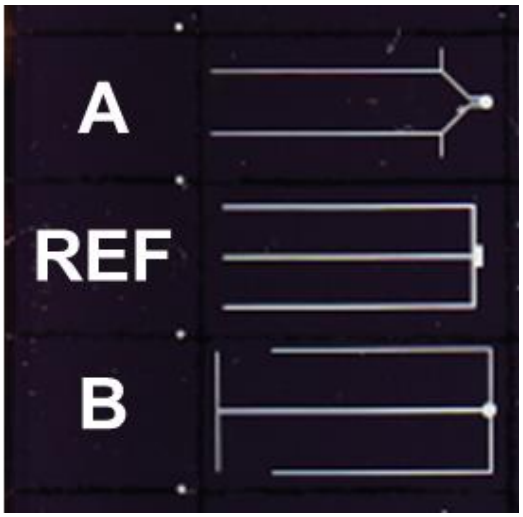

Figure 3: Picture of three solar cells metallic contacts realized by shadow masks. REF: Reference contact, A, B contacts obtained by automatic contact optimization.

Two contacts were selected for being realized experimentally, these are marked with red dots and letters in Fig. 2. The shape of these two contacts together with the reference contact is shown in Fig. 3. Each contact geometry was prepared 6 times on each substrate totaling to 18 cells on each substrate. Two substrates were fabricated: one with a TCO thickness of 200 nm and the second with a TCO thickness of 100 nm thus leading to four different combinations of contact shape and TCO.

Table I: Summary of the absolute efficiency losses calculated for the contact types being studied.

	Ohmic losses	Shadow losses	Total losses
REF	0.2 %	1.0 %	1.2 %
A	0.4 %	0.5 %	0.9 %
B	0.2 %	0.7 %	0.9 %

The absolute loss of efficiency due to ohmic losses and shadowing losses expected for each type of contact can be easily calculated by the FEM tool and a summary is shown in Table I. Additionally, the distribution of the electric potential on the cell surface when the cell is operating at the maximum power point (MPP) is an indication of ohmic losses. In the ideal case of a perfectly conducting TCO and metal grid, the potential on

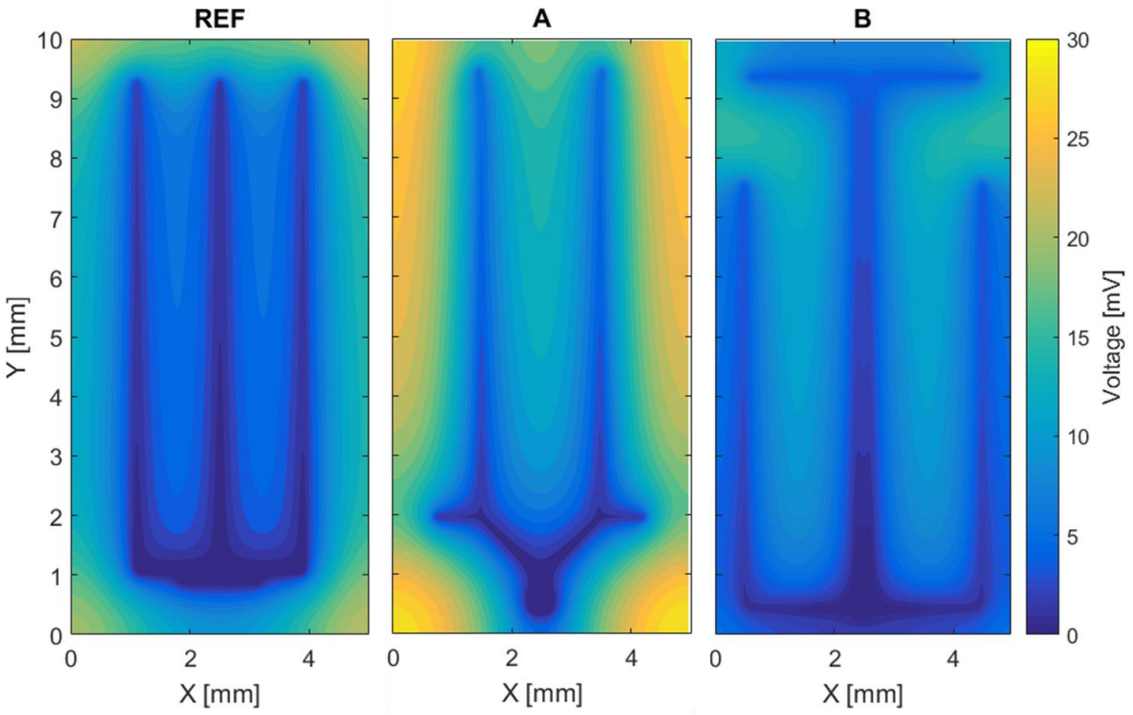

Figure 4: Potential difference distributions on the top TCO for the three contact types being studied. The maximum potential difference from V_{MPP} is 24 mV for the reference contact, 29 mV for the contact A and 15 mV for the contact B.

the whole cell surface corresponds to the voltage at MPP (V_{MPP}). In the presence of ohmic losses the cell surface will have an higher potential than the external contact at $V_{MPP.}$ As an example, the potential differences distributions above V_{MPP} in the three contact types being studied are shown in Fig. 4.

The comparison of predicted and measured changes in R_{ser} and J_{sc} are shown in Fig. 5. The prediction of R_{ser} agrees well with the experimental results thus confirming the validity of this approach to optimize contact geometries.

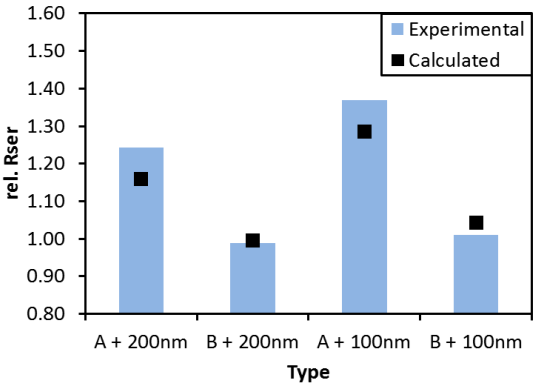

Figure 5: Comparison of calculated relative R_{ser} and measured relative R_{ser} for the different contact types being studied.

Similarly, the relative J_{sc} predicted by simulations and the experimentally measured relative J_{sc} are shown in Fig. 6. The agreement is again good except the first case of contact A combined with 200 nm TCO. The disagreement in the first case is not yet well understood, but it seems to be independent of the contact geometry as the second set of cells produced with the same shadow mask does not show such a large deviation.

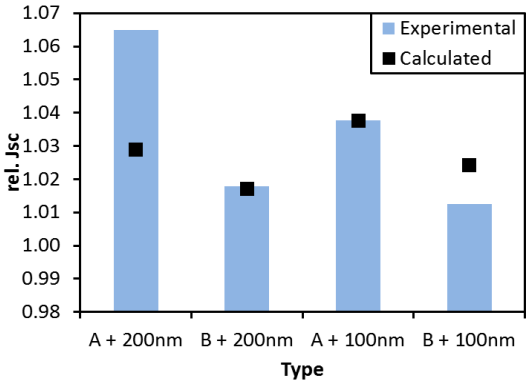

Figure 6: Comparison of calculated relative Jsc and measured relative Jsc for the different contact types being studied.

Finally the absolute gain in efficiency which can be achieved using the optimized contacts is shown in Fig. 7. The cells with 200 nm TCO show a good agreement between simulated gain and experimental gain. However, all cells with thin TCO including the references are affected by a drop of performance which is not fully understood; therefore the agreement is poor in this case.

The simulated improvements indicate an advantage of contacts achieving an improvement of R_{ser}: such contacts can be combined with a thinner TCO to reduce parasitic losses but still obtain a net increase of efficiency. Combining detailed FEM simulations with contact optimization and optical simulations allows to quickly find an optimum combination of TCO thickness and contact shape.

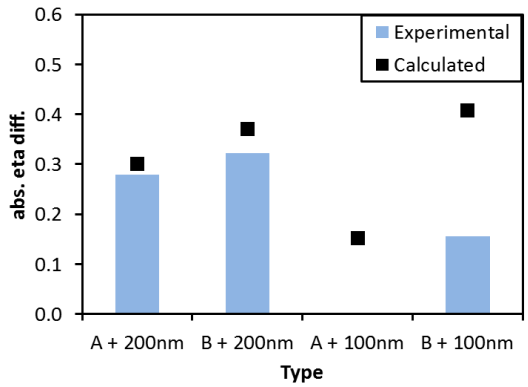

Figure 7: Comparison of calculated absolute increase in efficiency with measured absolute increase of efficiency for the different contact types being studied.

4 CONCLUSIONS

Automatic optimization of metallic contacts has been shown to be able to improve the cell performance compared to reference contacts and the predictions by 2D + 1D FEM simulations can be reliably used to design contacts and optimize solar cells. The method can be used to optimize larger area solar cells and solar modules. Additionally, it can be applied to other PV technologies.

5 ACKNOWLEDGEMENTS

The research leading to these results has received funding from the Swiss Competence Center for Energy and Mobility and from the Swiss Federal Office of Energy (project CONNECT-PV). The authors would like to thank G. Sartoris for useful discussions and valuable advice.

6 REFERENCES

[1] A. Chirilă, S. Buecheler, F. Pianezzi, P. Bloesch, C. Gretener, A.R. Uhl, C. Fella, L. Kranz, J. Perrenoud, S. Seyrling, R. Verma, S. Nishiwaki, Y.E. Romanyuk, G. Bilger, A.N. Tiwari, Highly efficient Cu(In,Ga)Se2 solar cells grown on flexible polymer films, Nat. Mater. 10 (2011) 857–861. doi:10.1038/nmat3122.

[2] K. Brecl, M. Topič, F. Smole, A detailed study of monolithic contacts and electrical losses in a large-area thin-film module, Prog. Photovolt. Res. Appl. 13 (2005) 297–310. doi:10.1002/pip.589.

[3] K. Brecl, M. Topič, Simulation of losses in thin-film silicon modules for different configurations and front contacts, Prog. Photovolt. Res. Appl. 16 (2008) 479–488. doi:10.1002/pip.831.

[4] T. Lanz, M. Bonmarin, M. Stuckelberger, C. Schlumpf, C. Ballif, B. Ruhstaller, Electrothermal Finite-Element Modeling for Defect Characterization in Thin-Film Silicon Solar Modules, IEEE J. Sel. Top. Quantum Electron. 19 (2013) 1–8. doi:10.1109/JSTQE.2013.2250259.

[5] J. van Deelen, L. Klerk, M. Barink, Optimized grid design for thin film solar panels, Sol. Energy. 107 (2014) 135–144. doi:10.1016/j.solener.2014.05.028.

[6] F.W. Fecher, A. Pérez Romero, C.J. Brabec, C. Buerhop-Lutz, Influence of a shunt on the electrical behavior in thin film photovoltaic modules – A 2D finite element simulation study, Sol. Energy. 105 (2014) 494–504. doi:10.1016/j.solener.2014.04.011.

[7] Y. Gupta, H. Liers, S. Woods, S. Young, R. DeBlasio, L. Mrig, Optimization of a-si solar cell current collection, in: Proc. 16th IEEE Photovolt. Spec. Conf., IEEE, San Diego, USA, 1982: pp. 1092–1101.

[8] H. B. Serreze, Optimizing Solar Cell Performance by Simultaneous Consideration of Grid Pattern Design and Interconnect Configurations, in: 1978: pp. 1–8.

[9] Y. Galagan, E.W.C. Coenen, S. Sabik, H.H. Gorter, M. Barink, S.C. Veenstra, J.M. Kroon, R. Andriessen, P.W.M. Blom, Evaluation of ink-jet printed current collecting grids and busbars for ITO-free organic solar cells, Sol. Energy Mater. Sol. Cells. 104 (2012) 32–38. doi:10.1016/j.solmat.2012.04.039.

[10] G. Sartoris, et al., NM-SESES, Numerical Modelling, 2016. http://nmtec.ch/nm-seses/documentation.

[11] G.P. Steven, Q. Li, Y.M. Xie, Evolutionary topology and shape design for general physical field problems, Comput. Mech. 26 (2000) 129–139. doi:10.1007/s004660000160.

[12] A. Chirilă, P. Reinhard, F. Pianezzi, P. Bloesch, A.R. Uhl, C. Fella, L. Kranz, D. Keller, C. Gretener, H. Hagendorfer, D. Jaeger, R. Erni, S. Nishiwaki, S. Buecheler, A.N. Tiwari, Potassium-induced surface modification of Cu(In,Ga)Se2 thin films for high-efficiency solar cells, Nat. Mater. 12 (2013) 1107–1111. doi:10.1038/nmat3789.